The Chiral Separation Effect in quenched finite-density QCD

Matthias Puhr[1],[★] and *Pavel* Buividovich[1]

[1]*Institute of Theoretical Physics, Regensburg University, 93040 Regensburg, Germany*

Abstract. We present results of a study of the Chiral Separation Effect (CSE) in quenched finite-density QCD. Using a recently developed numerical method we calculate the conserved axial current for exactly chiral overlap fermions at finite density for the first time. We compute the anomalous transport coefficient for the CSE in the confining and deconfining phase and investigate possible deviations from the universal value. In both phases we find that non-perturbative corrections to the CSE are absent and we reproduce the universal value for the transport coefficient within small statistical errors. Our results suggest that the CSE can be used to determine the renormalisation factor of the axial current.

1 Motivation and Introduction

In heavy-ion collision experiments it is possible to generate densities and temperatures that are comparable to the conditions in the early universe. These experiments are an important tool to study open questions in cosmology, astrophysics and high-energy physics. The hot and dense plasma generated in heavy-ion collisions is dominated by quarks and gluons. QCD is an asymptotically free theory and at high enough temperatures and densities one expects that the quarks and gluons become deconfined. If the collisions are off-centre very large magnetic fields can be generated [1–3]. For these reasons one can expect that anomalous transport phenomena [4, 5] might play a role in heavy-ion collision experiments and it is of great interest to study anomalous transport in QCD.

Prominent examples of anomalous transport phenomena are the induction of an axial or vector current parallel to an external magnetic field in a dense chiral medium, the so-called Chiral Separation effect (CSE) [6–9] and Chiral Magnetic effect (CME) [10, 11], respectively. In combination the CSE and the CME can give rise to a gap-less hydrodynamic mode, the Chiral Magnetic Wave [12, 13]. For reviews about the experimental signatures of anomalous transport effects see for example [4, 5].

Because of their relation to the axial anomaly it has been argued that the anomalous transport coefficients are universal and do not get any corrections in interacting theories. Closer investigations revealed, however, that there are two scenarios where corrections to the anomalous transport coefficients can occur: If chiral symmetry is spontaneously broken [14–16] and in an unquenched theory if the currents couple to dynamical gauge fields [17–19].

The focus of this work is the CSE in QCD, where non-perturbative corrections to the transport coefficient can be expressed in terms of the in-medium amplitude $g_{\pi^0\gamma\gamma}$ of the decay $\pi^0 \to \gamma\gamma$ [14]:

$$j_i^5 = \sigma_{\text{CSE}} B_i, \quad \sigma_{\text{CSE}} = \sigma_{\text{CSE}}^0 \left(1 - g_{\pi^0\gamma\gamma}\right), \tag{1}$$

[★]Speaker, e-mail: matthias.puhr@physik.uni-regensburg.de

where j_i^5 is the axial current density and B_i the external magnetic field. In the limit $g_{\pi^0\gamma\gamma} \to 0$ the transport coefficient σ_{CSE} reduces to the value for free chiral quarks σ_{CSE}^0. For a single quark flavour with N_c colour degrees of freedom it is given by

$$\sigma_{\text{CSE}}^0 = \frac{qN_c\mu}{2\pi^2}, \tag{2}$$

where q is the electrical charge of the quark and μ the quark chemical potential.

In the linear sigma model $g_{\pi^0\gamma\gamma}$ can be calculated and in the phase with broken chiral symmetry (for sufficiently small chemical potential) it is given by $g_{\pi^0\gamma\gamma} = \frac{7\zeta(3)m^2}{4\pi^2T^2}$, where ζ is the Riemann ζ-function, m is the constituent quark mass and T is the temperature [14]. Plugging in the values $m \sim 300\,\text{MeV}$ and $T \sim 150\,\text{MeV}$, which give a realistic low-energy description of the chirally broken phase of QCD [20], we find a correction of order 100% which suppresses the CSE current. Corrections suppressing the CSE were also found in other model calculations [21–25].

For accurate predictions of signatures of anomalous transport effects in heavy-ion collision experiments it is desirable to gain a quantitative, model-independent understanding of possible corrections to the anomalous transport coefficients from first-principle lattice QCD simulations. Previous lattice studies looked at the infrared values of the anomalous transport coefficients for the CME [26, 27] and the Chiral Vortical Effect (CVE) [28, 29]. These studies found a significant suppression of the CME and the CVE at both low and high temperatures, conflicting with expectations based on the hydrodynamic approximation. At least at high temperatures the thermodynamic consistency arguments fixing the anomalous transport coefficients within this approximation should be valid [30, 31]. It is possible that the origin of this discrepancy lies in the use of a naively discretised non-conserved vector current [26, 27] and energy-momentum tensor [28, 29]. Moreover, the simulations in [26, 27] were performed with non-chiral Wilson–Dirac lattice fermions.

In this contribution we report on a first-principles lattice study of the CSE, previously published in [32]. To avoid unquantifiable systematic errors we work with finite-density overlap fermions [33], which respect a lattice version of chiral symmetry, and use the properly defined conserved lattice axial vector current density [34, 35]:

$$j_{x,\mu}^5 = \tfrac{1}{2}\bar{\psi}\left(-\gamma_5 K_{x,\mu} + K_{x,\mu}\gamma_5(1 - D_{\text{ov}})\right)\psi, \tag{3}$$

where $K_{x,\mu} = \frac{\partial D_{\text{ov}}}{\partial \Theta_{x,\mu}}$ is the derivative of the overlap operator D_{ov} over the $U(1)$ lattice gauge field $\Theta_{x,\mu}$. With the definition (3) the lattice axial current transforms covariantly under the lattice chiral symmetry. For vanishing bare quark mass it is therefore protected from renormalisation and can be directly related to the continuum axial current density $j_\mu^5 = \bar{\psi}\gamma_5\gamma_\mu\psi$, which enters Equation (1). Taking the expectation value of (3) and using the Ginsparg–Wilson equation to simplify the resulting expression finally yields

$$\langle j_{x,\mu}^5 \rangle = \text{tr}\left(D_{\text{ov}}^{-1}\frac{\partial D_{\text{ov}}}{\partial \Theta_{x,\mu}}\gamma_5\right). \tag{4}$$

Efficiently computing the derivatives $\frac{\partial D_{\text{ov}}}{\partial \Theta_{x,\mu}}$ with high accuracy is a non-trivial numerical problem and we developed a new numerical algorithm for this purpose. For details on the evaluation of the derivatives we refer the reader to [36].

2 Simulation parameters and numerical setup

Lattice QCD with dynamical fermions has a sign problem at finite quark chemical potential. In order to avert the sign problem we work in the quenched approximation and neglect the effects of sea quarks.

While calculations within a random matrix model show that the chiral condensate in quenched QCD vanishes and chiral symmetry is restored for any non-zero chemical potential [37], the presence of an external magnetic field can potentially change this picture. On the one hand random matrix theory is no longer applicable in this case and on the other hand non-perturbative corrections to the CSE due to the formation of a new type of condensate, the so-called chiral shift parameter [21–23], are possible.

The SU(3) gauge configurations are generated using the tadpole-improved Lüscher–Weisz gauge action [38]. We use three different parameter sets for our simulations: $V = L_T \times L_S^3 = 6 \times 18^3$ with $\beta = 8.45$ corresponding to a temperature $T > T_c$ and $V = 14 \times 14^3$ and $V = 8 \times 8^3$ with $\beta = 8.10$ corresponding to $T < T_c$, where L_T and L_S are the temporal and spatial extent of the lattice and $T_c \approx 300$ MeV is the deconfinement transition temperature of the Lüscher–Weisz action [39]. To fix the lattice spacing a we take the results from [40]. The values of all parameters in lattice and physical units are summarised in Table 1.

Setup	β	8.1	8.1	8.45
	Volume	14×14^3	8×8^3	6×18^3
	Lattice	Physical Value		
a [fm]	1	0.125	0.125	0.095
V_S [fm^3]	L_S^3	5.4	1.0	5.0
T [MeV]	L_T^{-1}	113	197	346
μ [MeV]	0.050	79	$\cdots$	$\cdots$
	0.100	$\cdots$	158	$\cdots$
	0.300	474	$\cdots$	$\cdots$
	0.040	$\cdots$	$\cdots$	83
	0.230	$\cdots$	$\cdots$	478
$\frac{qB}{\Phi_B}$ [MeV]^2	$\frac{2\pi}{a^2 L_S^2}$	283^2	495^2	289^2

Table 1: Simulation parameters

For the 6×18^3 and 14×14^3 lattices approximately 10^3 configurations were generated, from which we randomly picked 100 with topological charge $Q = 0$[1]. Additionally we chose 100 configurations with topological charge $|Q| = 1$ for $V = 6 \times 18^3$ and 111 with $|Q| = 1$ and 97 with $|Q| = 2$ for $V = 14 \times 14^3$. For the $V = 8 \times 8^3$ lattice $5 \cdot 10^3$ configurations were generated, from which we selected three random sets of 200 configurations with $Q = 0$, $|Q| = 1$ and $|Q| = 2$.

The topological charge of a given gauge configuration can be calculated by taking the difference of the number of left- and right-handed zero modes of the overlap operator: $Q = n_L - n_R$. In practice configurations with zero modes with both chiralities do not occur and the overlap operator always has either $n_R = |Q|$ right-handed or $n_L = |Q|$ left-handed zero modes (see e.g. Section 7.3.2 in [41]). Exploiting this fact we calculated the absolute value of the topological charge $|Q| = |n_R - n_L|$ as the number of zero eigenvalues of the operator $D_{\rm ov}D_{\rm ov}^\dagger$.

To introduce a constant, homogeneous external magnetic field on the lattice we follow [42] and introduce a magnetic flux quantum $\Phi_B = 1, 2, 5, 10$ for $V = 14 \times 14^3$ and $V = 6 \times 18^3$ at $Q = 0$, and $\Phi_B = 0, 1, 2, 3, 4$ for $V = 8 \times 8^3$ at all Q. For $V = 6 \times 18^3$ we chose $\Phi_B = 0, 1, 2, 3, 5$ at $|Q| = 1$ and $\Phi_B = 1, 3, 5, 8, 10$ for $V = 14 \times 14^3$ at $|Q| = 1, 2$. The axial current density is computed by averaging

---

[1]One of the configurations for the parameters $V = 14 \times 14^3$, $\beta = 8.1$, $\mu = 0.050$ and a magnetic flux of $\Phi_B = 1$ caused a serious breakdown in the Lanczos algorithm when computing the overlap operator and only the remaining 99 configurations were used for this parameter set.

(4) over all lattice sites x. To evaluate the trace we use the stochastic estimator technique with Z_2-noise. The number of stochastic estimators is increased until the results are stable. The axial current density is only well defined if the overlap operator is invertible, i.e., if $Q = 0$. Working exclusively on configurations with $Q = 0$ introduces an systematic error and in order to perform a cross-check of our results we also consider configurations with $|Q| > 0$. Since the computations are numerically very expensive, we only do the cross-checks for a single value of the chemical potential. By introducing a small finite quark mass $m_q = 0.001 \, a^{-1}$ on configurations with non-zero topological charge we make the overlap operator invertible. Strictly speaking the axial current defined via Equation (4) is no longer protected from renormalisation in this case. To demonstrate that the effect of the finite quark mass on σ_{CSE} is negligible in practice, we consider a second mass value $m_q = 0.002 \, a^{-1}$ for the $V = 8 \times 8^3$ configurations.

The value of σ_{CSE} is given by the slope of the axial current density as a function of the external magnetic field. We extract σ_{CSE} from our axial current data by performing a one parameter linear fit. Confidence intervals for σ_{CSE} are calculated with the statistical bootstrap method: For every bootstrap sample we first independently draw 100 configurations for every value of Φ_B and then perform a fit to the data generated in this way.
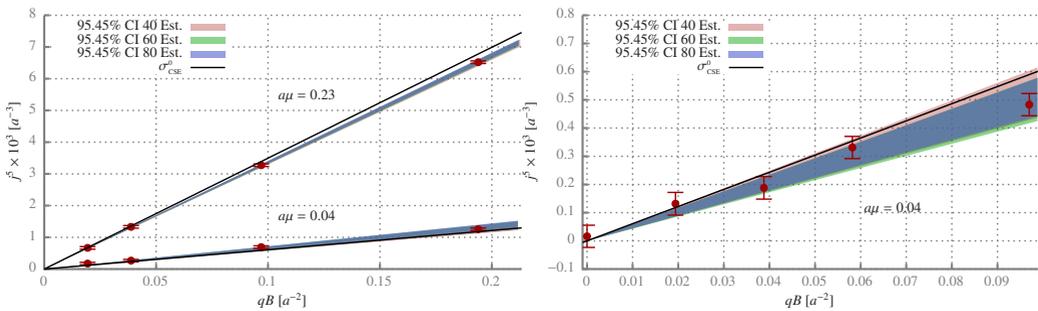

Figure 1: The axial current density j^5 as a function of the magnetic field strength B for $T < \mathrm{T_c}$. The left plot shows results for $Q = 0$ and on the right $|Q| = 1$ (note the different scales). The red dots with errorbars are our data and the shaded regions mark the bootstrap confidence intervals for σ_{CSE} for a different number of stochastic estimators. Solid black lines correspond to the free fermion result σ_{CSE}^0.

3 Results

First we present results for the high-temperature deconfinement phase, where $T = 346 \, \mathrm{MeV} > T_c$. Here the chiral symmetry should be restored[2] and we expect that there are no corrections to the CSE current [7, 14, 45]. Our data is plotted in Figure 1 and as expected in general we find good agreement with the free fermion result σ_{CSE}^0. The sole exception is the data point for $Q = 0$, $\mu = 0.230 \, a^{-1}$ and $\Phi_B = 10$, where we might see the onset of saturation. To make sure that our results for σ_{CSE} are not affected by possible statuartion effects, we additionally perform fits where the data for the largest value of Φ_B is left out (see Figure 2a).

Next we examine the results for the low-temperature confinement phase, where non-perturbative corrections to the CSE are expected. As a proof of concept we first consider the small $V = 8 \times 8$ lattice. In the topological sector $Q = 0$ we again find a very good agreement with σ_{CSE}^0, but for $|Q| \neq 0$

---

[2]The restoration of chiral symmetry in the deconfinement phase of quenched lattice QCD is discussed, e.g., in [43, 44]
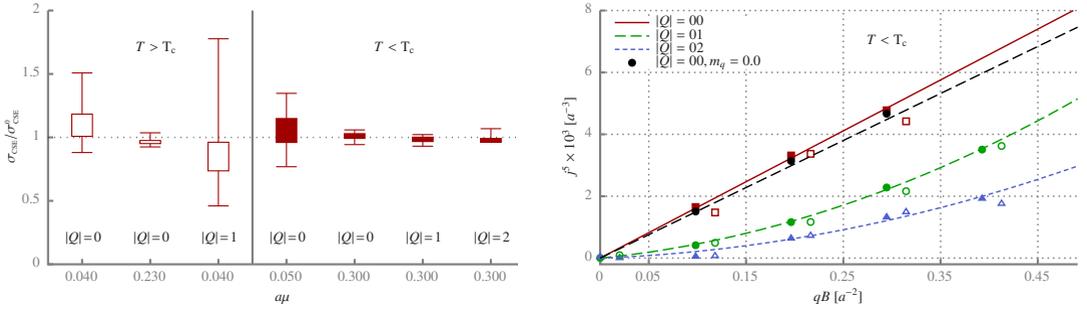
(a) Summary of the results for the confidence intervals for the ratio $\sigma_{\text{CSE}}/\sigma_{\text{CSE}}^0$ for the lattices with $V = 14 \times 14^3$ and $V = 6 \times 18^3$. Results for $T > T_c$ and $T < T_c$ are marked by open and closed boxes, respectively. The boxes denote the results of a fit to all data points and the whiskers show the results if the data for the largest value of Φ_B are excluded.

(b) The axial current density j^5 in different topological sectors for the $V = 8 \times 8^3$ lattice. The results for $m_q = 0.001 \, a^{-1}$ are denoted by filled symbols, the data for $m_q = 0.002 \, a^{-1}$ are shifted by $0.02 \, a^{-2}$ in the qB axis for better visibility and are marked by open symbols. The black dots show the axial current with $Q = 0$ for vanishing quark mass and the black dashed line corresponds to the free fermion result σ_{CSE}^0. To guide the eye a linear ($Q = 0$) or second order polynomial ($|Q| > 0$) fit to the data is shown.

Figure 2

there are large deviations from the free fermion result. The results for different bare quark masses lie on top of each other and we conclude that for small quark masses the renormalisation of the axial current is negligible.

A lattice volume of $V = 8 \times 8^3$ is very small and to check for finite size effects we also perform simulations for $V = 14 \times 14^3$. The results for the larger lattice are shown in Figure 3. The data for $Q = 0$ is in very good agreement with the results for the smaller lattice size and there does not seem to be a large finite size effect for this topological sector. For the $|Q| \neq 0$ sectors the picture is completely different: Contrary to the small volume calculations the CSE current does not get any corrections. The plots in Figure 3 clearly show that for the larger lattice volume the data for all topological sectors and chemical potentials we investigated are in perfect agreement with the free fermion result σ_{CSE}^0. A possible reason for the large finite size effects in topological sectors with non-zero Q is discussed in [32]. The results for all our simulations on larger lattices are summarised in Figure 2a.

4 Conclusion

We performed a numerical study to quantify possible non-perturbative corrections to the CSE current in quenched lattice QCD. Within statistical errors, which are smaller than 10% for the simulations with larger chemical potentials (see Figure 2a), we do not find any correction to the CSE current and reproduce the free fermion value σ_{CSE}^0 for the transport coefficient. The use of finite-density overlap fermions and a conserved lattice axial current, which transforms covariantly under the lattice chiral symmetry, eliminates potential systematic errors due to a explicit breaking of chiral symmetry or a renormalisation of the axial current. Comparing the results for different lattice sizes suggest that finite size effects are very small, at least in the topological sector $Q = 0$. A remaining source of systematic errors is the quenched approximation. Taking the results of the random matrix model [37] at face value, one could argue that the chiral condensate in quenched QCD should vanish as soon as
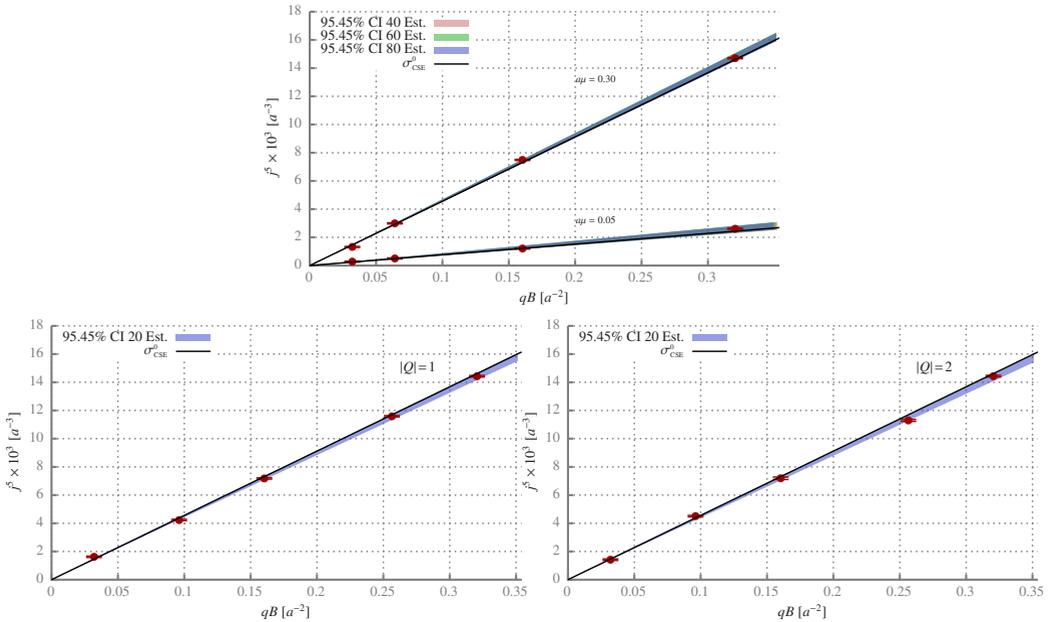
Figure 3: The axial current density j^5 as a function of the magnetic field strength B in different topological sectors for the lattice with $V = 14 \times 14^3$ at $T < T_c$ (red dots with errorbars). In the plot on the top $Q = 0$, $|Q| = 1$ on the bottom left plot and on the bottom right $|Q| = 2$. Solid black lines denote the free fermion result σ^0_{CSE} and shaded regions mark the confidence intervals for σ_{CSE}.

a finite chemical potential is turned on and consequently the non-perturbative corrections predicted for the phase with broken chiral symmetry should be absent. However, on the one hand the random matrix calculation can not take into account a finite external magnetic field and on the other hand the presence of such a field can instigate the spontaneous formation of condensates, like the chiral shift parameter of [21–23], which can also give non-perturbative corrections to the CSE. Moreover, the holographic calculations [24, 25] found non-perturbatice corrections to the CSE at small temperatures and were done in the quenched approximation (or "probe limit" in the language of AdS/CFT). For all this reasons the non-renormalisation of the CSE current in quenched QCD at both high and low temperatures is a non-trivial result.

It is important to emphasise that the results for the quenched theory do not necessarily generalise to full QCD. In particular, our results do not exclude possible corrections that could have their origin in the complex phase that the fermion determinate acquires at finite chemical potential. Note that unquenched lattice calculations of the CSE are notoriously difficult, since the necessity to introduce an external magnetic field leads to a complex fermion determinant even in gauge theories which do otherwise not have a sign problem at finite chemical potential, like for example SU(2) and G_2 gauge theories.

The non-renormalisation of the CSE in quenched QCD has a potential practical application: If the axial current is computed for non-chiral lattice fermions and/or with a non-covariant discretisation of the axial current, the ratio of this current and the exact result $j^5_i = \sigma^0_{CSE} B_i$ gives the multiplicative renormalisation constant for the axial current for this particular lattice discretisation of the Dirac operator and axial current.

Acknowledgements

References

[1] D.E. Kharzeev, L.D. McLerran, H.J. Warringa, Nucl. Phys. A **803**, 227 (2008), `0711.0950v1`
[2] V. Skokov, A. Illarionov, V. Toneev, Int. J. Mod. Phys. A **24**, 5925 (2009), `0907.1396v1`
[3] L. McLerran, V. Skokov, **929**, 184 (2014), `1305.0774`
[4] D.E. Kharzeev, J. Liao, S.A. Voloshin, G. Wang, Prog. Part. Nucl. Phys. **88**, 1 (2016), `1511.04050`
[5] J. Liao, Nucl. Phys. A **956**, 99 (2016), `1601.00381v1`
[6] D.T. Son, A.R. Zhitnitsky, Phys. Rev. D **70**, 074018 (2004), `hep-ph/0405216`
[7] M.A. Metlitski, A.R. Zhitnitsky, Phys. Rev. D **72**, 045011 (2005), `hep-ph/0505072`
[8] D.T. Son, Phys. Rev. B **75**, 235423 (2007), `cond-mat/0701501`
[9] D. Kharzeev, A. Zhitnitsky, Nucl. Phys. A **797**, 67 (2007), `0706.1026`
[10] A. Vilenkin, Phys. Rev. D **22**, 3080 (1980)
[11] K. Fukushima, D.E. Kharzeev, H.J. Warringa, Phys. Rev. D **78** (2008), `0808.3382`
[12] Y. Burnier, D.E. Kharzeev, J. Liao, H.U. Yee, Phys. Rev. Lett. **107**, 052303 (2011), `1103.1307v1`
[13] D.E. Kharzeev, H.U. Yee, Physical Review D **83**, 085007 (2011), `1012.6026v2`
[14] G.M. Newman, D.T. Son, Physical Review D **73**, 045006 (2006), `hep-ph/0510049`
[15] P.V. Buividovich, Nucl. Phys. A **925**, 218 (2014), `1312.1843`
[16] P.V. Buividovich, Phys. Rev. D **90**, 125025 (2014), `1408.4573v2`
[17] K. Jensen, P. Kovtun, A. Ritz, JHEP **2013**, 186 (2013), `1307.3234v1`
[18] E.V. Gorbar, V.A. Miransky, I.A. Shovkovy, X. Wang, Phys. Rev. D **88**, 025025 (2013), `1304.4606`
[19] U. Gursoy, A. Jansen, JHEP **2014**, 092 (2014), `1407.3282v2`
[20] L.R. Baboukhadia, V. Elias, M.D. Scadron, J. Phys. G: Nucl. Part. Phys. **23**, 1065 (1997), `hep-ph/9708431`
[21] E.V. Gorbar, V.A. Miransky, I.A. Shovkovy, Phys. Rev. C **80**, 032801 (2009), `0904.2164v2`
[22] E.V. Gorbar, V.A. Miransky, I.A. Shovkovy, Phys. Lett. B **695**, 354 (2011), `1009.1656v2`
[23] E.V. Gorbar, V.A. Miransky, I.A. Shovkovy, Phys. Rev. D **83** (2011), `1101.4954v2`
[24] I. Amado, N. Lisker, A. Yarom, JHEP **2014** (2014), `1401.5795`
[25] A. Jimenez-Alba, L. Melgar, JHEP **2014** (2014), `1404.2434v3`
[26] A. Yamamoto, Phys. Rev. Lett. **107**, 031601 (2011), `1105.0385`
[27] A. Yamamoto, **84**, 114504 (2011), `1111.4681`
[28] V. Braguta, M.N. Chernodub, K. Landsteiner, M.I. Polikarpov, M.V. Ulybyshev, Physical Review D **88**, 071501 (2013), `1303.6266v2`
[29] V. Braguta, M.N. Chernodub, V.A. Goy, K. Landsteiner, A.V. Molochkov, M.I. Polikarpov, Phys. Rev. D **89**, 074510 (2014), `1401.8095v1`
[30] D.T. Son, P. Surowka, Phys. Rev. Lett. **103**, 191601 (2009), `0906.5044`

[31] A.V. Sadofyev, M.V. Isachenkov, Phys. Lett. B **697**, 404 (2011), `1010.1550`

[32] M. Puhr, P. Buividovich, Phys. Rev. Lett. **118**, 192003 (2016), `1611.07263v3`

[33] J. Bloch, T. Wettig, **97**, 012003 (2006), `hep-lat/0604020`

[34] P. Hasenfratz, S. Hauswirth, T. Jörg, F. Niedermayer, K. Holland, Nucl. Phys. B **643**, 280 (2002), `hep-lat/0205010`

[35] Y. Kikukawa, A. Yamada, Nucl. Phys. B **547**, 413 (1999), `hep-lat/9810024`

[36] M. Puhr, P. Buividovich, Comput. Phys. Commun. **208**, 135 (2016), `1604.08057`

[37] M.A. Stephanov, Physical Review Letters **76**, 4472 (1996), `hep-lat/9604003v2`

[38] M. Lüscher, P. Weisz, Communications in Mathematical Physics **97**, 59 (1985)

[39] C. Gattringer, P.E.L. Rakow, A. Schaefer, W. Soeldner, Phys. Rev. D **66**, 054502 (2002), `hep-lat/0202009v1`

[40] C. Gattringer, R. Hoffmann, S. Schaefer, Phys. Rev. D **65** (2002), `hep-lat/0112024`

[41] C. Gattringer, C.B. Lang, *Quantum Chromodynamics on the Lattice* (Springer Berlin Heidelberg, 2010)

[42] M.H. Al-Hashimi, U.J. Wiese, Ann. Phys. **324**, 343 (2009), `0807.0630v1`

[43] R.G. Edwards, U.M. Heller, J. Kiskis, R. Narayanan, Physical Review D **61**, 074504 (2000), `hep-lat/9910041v1`

[44] J. Kiskis, R. Narayanan, Physical Review D **64**, 117502 (2001), `hep-lat/0106018v2`

[45] A.Y. Alekseev, V.V. Cheianov, J. Froehlich, Phys. Rev. Lett. **81**, 3503 (1998), `cond-mat/9803346`